Optics Letters

Hundred-meter-scale, kilowatt peak-power, near-diffraction-limited, mid-infrared pulse delivery via the low-loss hollow-core fiber

Qiang Fu,[1,*] Yudi Wu,[1] Ian A. Davidson,[1] Lin Xu,[1,2] Gregory T. Jasion,[1] Sijing Liang,[1] Shuichiro Rikimi,[1] Francesco Poletti,[1] Natalie V. Wheeler,[1] and David J. Richardson[1]

[1]Optoelectronics Research Centre, University of Southampton, Southampton, SO17 1BJ, UK
[2]e-mail: L.Xu@soton.ac.uk
*Corresponding author: Qiang.Fu@soton.ac.uk

Received 16 August 2022; revised 15 September 2022; accepted 19 September 2022; posted 20 September 2022; published 6 October 2022

We report a high-power single-mode mid-infrared (MIR) pulse delivery system via anti-resonant hollow-core fiber (HCF) with a record delivery distance of 108 m. Near-diffraction-limited MIR light was transmitted by HCFs at wavelengths of 3.12–3.58 μm using a tunable optical parametric oscillator (OPO) as the light source. The HCFs were purged beforehand with argon in order to remove or reduce loss due to parasitic gas absorption (HCl, CO_2, etc.). The minimum fiber loss values were 0.05 and 0.24 dB/m at 3.4–3.6 μm and 4.5–4.6 μm, respectively, with the 4.5–4.6 μm loss figure representing, to the best of our knowledge, a new low loss record for a HCF in this spectral region. At a coupling efficiency of ~70%, average powers of 592 mW and 133 mW were delivered through 5 m and 108 m of HCF, respectively. Assuming the 120-ps duration of the MIR pulses remained constant over the low-dispersion HCF (theoretical maximum: 0.4 ps/nm/km), the corresponding calculated peak powers were 4.9 kW and 1.1 kW.

https://doi.org/10.1364/OL.473230

Long-distance, fiber-based, single-mode laser beam delivery systems could open up unprecedented possibilities for diverse applications of current and emerging high-power laser sources. For instance, kilowatt-power, single-mode near-infrared laser beams have now been successfully transmitted over kilometer distances, making them suitable for future industrial manufacturing in giga-factories and subsurface rock drilling, amongst other applications [1]. In the MIR spectral region, there is also a growing drive for such laser delivery systems, for example, in the processing of organic materials [2–4], spectroscopy [5], biomedical diagnostics [6], and surgical treatment [7,8]. In laser surgery, for example, optical fibers enhance system flexibility and allow the placement of the laser source far from the operating theater, freeing up space for surgeons and enabling a safer and less cluttered operating environment.

Traditional silica solid-core fibers are not viable for MIR light transmission at wavelengths longer than 2.5 μm due to high material absorption. Alternative materials such as heavy metal oxide glass, fluoride glass, and chalcogenide glass have therefore been investigated and various MIR fibers have been fabricated over the past decades [9]. However, fabrication difficulties have significantly hindered the production of long lengths of fiber and hence applications requiring long-distance MIR laser delivery. Current delivery distances have been limited to a few meters' length [10–14]. Moreover, the low damage thresholds, small mode areas, and high nonlinearity of these fibers are also a hindrance to their use in high-power single-mode MIR beam delivery.

Hollow-core fibers (HCFs) offer a radically new solution by guiding light in their hollow (typically air-filled) cores, leading to a high damage threshold and remarkably low nonlinearity, dispersion, and backscattering, making them highly suitable for MIR delivery. There are a few common types of MIR HCFs: metallic fibers [15], dielectric-coated Bragg (OmniGuide) fibers [16], photonic bandgap fibers [17], and antiresonant fibers [18]. Metallic fibers are somewhat outdated due to their mechanical rigidity, high loss, and multimode output [19]. Bragg fibers have a dielectric multilayered structure, leading to omnidirectional reflectivity. Although such fibers with a design for CO_2 laser transmission have gained a solid foothold for applications in surgery, their fiber length and potential operation at other MIR wavelengths are still held back by their challenging fabrication processes, where at least two thermomechanically compatible, high refractive-index contrast materials capable of being drawn down to fiber while reliably maintaining a multilayer structure with micrometer dimensions must be identified [9].

Hollow-core photonic bandgap fibers (HC-PBGFs) have a two-dimensional periodic structure, typically fabricated with silica glass, that creates a photonic bandgap that guides light. To date, HC-PBGFs have been reported with MIR transmission windows extending out to 3.7 μm and a minimum loss of

0.05 dB/m at 3.3 μm but with a relatively narrow transmission window of 0.6 μm in a 50-μm fiber core [17]. Although such fibers are of interest in MIR delivery, there are only a few reports of delivery experiments, and these have been over relatively short lengths of fiber. For example, Urich *et al*. demonstrated 0.4-m-distance MIR delivery of 62-W-peak-power, 225-μs-duration pulses at 2.94 μm from an Er:YAG laser in a 24-μm-core HC-PBGF with a low coupling efficiency of just 5% [20].

Hollow-core anti-resonant fibers (HC-ARFs) form an emerging subset of the HCF family, and have sparked great interest in MIR transmission, as chalcogenide-based HC-ARFs show guidance up to ~10 μm, coinciding with CO_2 laser emission wavelengths [21,22]. However, the fabrication of long lengths of soft-glass HC-ARFs is difficult, similar to the aforementioned solid-core, soft-glass fibers. Moreover, such fibers typically cannot withstand high temperatures and are relatively difficult to handle due to their low mechanical strength, limiting their suitability for industrial and medical applications. In contrast, silica-based HC-ARFs can be considered an excellent alternative, and have been reported to guide MIR light up to 7.9 μm [23]. Such fibers have high mechanical and chemical stability and are compatible with existing well-developed fabrication methods capable of producing long lengths of high-quality fiber for telecommunications applications; hence, they are suitable for long-distance MIR delivery. In a recent report, Urich *et al*. presented 9.88-m-maximum-distance MIR delivery of 0.24-kW-peak-power (54-mJ-pulse-energy) 2.94-μm laser pulses using a 0.034-dB/m-loss "ice-cream cone" HC-ARF design at a coupling efficiency of 35% [24]. Overall, current MIR HCF delivery systems are limited by difficulties in the fabrication of long lengths of compatible uniform low-loss single-mode fibers and the lack of stable, high-beam-quality, powerful MIR laser sources, which thus limits the possibilities for high-brightness output over long distances.

Here, we report the first hundred-meter-length-scale HCF delivery in the MIR wavelength range. A single-mode MIR beam is delivered 108 m through a purged HC-ARF with a transmitted maximum average power (peak power) of 133 mW (1.1 kW) at 3.3 μm and a coupling efficiency of ~70%. The fiber used has broadband low loss covering the wavelength region from 2.7 to 4.7 μm, with a minimum loss of 0.05 dB/m between 3.4 and 3.6 μm. MIR delivery was demonstrated between 3.12 and 3.58 μm using a wavelength-tunable, MIR, narrowband OPO laser source. The transmitted beams were near diffraction limited, with beam qualities of $M_x^2 = 1.02$ and $M_y^2 = 1.03$. We believe that this HCF-based MIR delivery technique has good potential for use in applications such as photothermal gas sensing within the HCF. It can leverage the combination of the fundamental resonances of important gas molecules, which lie within the MIR region, and the long gas–light interaction lengths possible in HCFs, which can serve to enhance sensitivity.

The MIR fiber is an in-house-made single-cladding ring ("tubular") HC-ARF, fabricated using Heraeus F300 fused silica glass via a two-step stack-and-draw technique [25]. A scanning electron microscope (SEM) cross-sectional image of the HC-ARF is shown in Fig. 1(a). The fiber has a core diameter of 105 μm, defined by seven capillaries with average inner diameters and membrane thicknesses of ~46.7 μm and ~1.08 μm, respectively. The fiber structure was specifically designed for delivering the laser beam from our high-power MIR OPO [26]. For example, the membrane thickness was selected to provide a broad fundamental guidance window that widely covered the OPO wavelength tuning range. According to our modeling, the design represents an excellent compromise between low fundamental mode loss (for efficient throughput), low bend sensitivity (for practical use), and good high-order mode suppression (to ensure effectively single-mode transmission). To characterize the fiber, an off-axis parabolic gold-coated mirror (RFL = 76.2 mm) was used to focus a collimated 0.8–4.8 μm supercontinuum laser beam (ELECTRO MIR4.8, Leukos Laser) into the fiber, which was coiled on a 32-cm-diameter drum. In the transmission spectrum of the 118-m fiber, HCl gas absorption features at ~3.2–3.8 μm were observed (not shown), indicating high fiber losses at corresponding wavelengths. These are common effects observed in long lengths of unpurged HCF due to the use of chlorine in the glass manufacturing process [17,18]. To eradicate HCl absorption features, the fiber was purged with 7.7-bar argon for 2 days, which is sufficient to replace all the gas in the 118-m HC-ARF (estimated from the gas flow model in [27]). After purging, the fiber was left open to the atmosphere (for ~6 hours) in order to eliminate unequal longitudinal overpressure inside the fiber, i.e., to equalize the gas pressures in both the fiber core and the cladding to atmospheric pressure. Such operation can avoid transient changes in the purged fiber's optical properties [28]. A cutback transmission/loss measurement was then conducted by cutting back from 118 m to 10 m, as shown in Fig. 1(b). The transmission spectra were recorded by a grating-based MIR monochromator (Bentham Instruments, TMc 300 V) at a resolution of 10 nm. Thanks to the argon purging, there are no HCl gas absorption features at ~3.2–3.8 μm. No evidence of re-emergence of HCl absorption features was observed after >100 hours of exposure of the argon-purged 108-m HC-ARF to the ambient atmosphere. In the transmission spectra shown in Fig. 1(b), CO_2 gas absorption features can be observed between

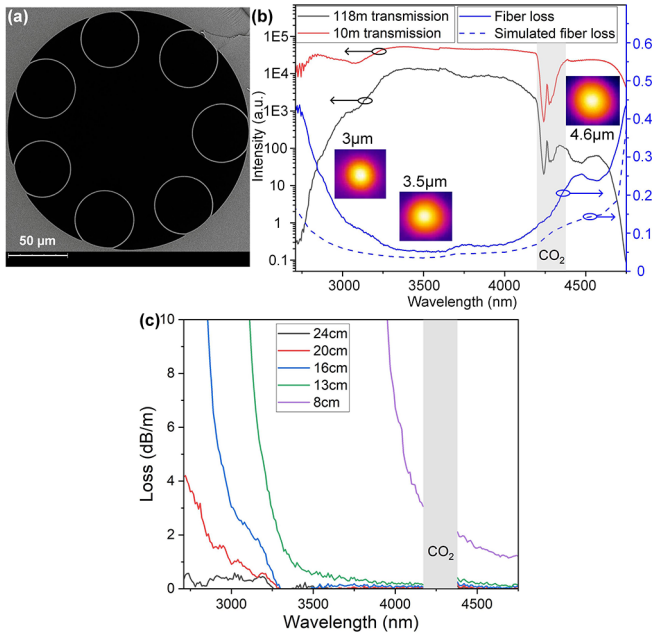

Fig. 1. (a) SEM image of the fiber cross section. (b) 10-m (red) and 118-m (black) HC-ARF transmission, experimental cutback loss (solid blue), and simulated fiber loss (dashed blue). Inset: 10-m HCF output beam profiles at wavelengths of 3, 3.5, and 4.6 μm. (c) HC-ARF macrobend loss measurement at bend diameters of 8, 13, 16, 20, and 24 cm.

4.2 and 4.3 μm (gray-shaded area), originating from the free-space coupling path, the beam path in the monochromator, and potentially CO_2 ingress into the unsealed purged fiber. From the cutback measurement, the fiber has a broadband low-loss window extending from 2.7 to 4.7 μm, and the minimum loss value of 0.05 dB/m is obtained between 3.4 and 3.6 μm. It should be noted that the loss of ~0.24 dB/m between 4.5 and 4.6 μm represents a new record for a HCF in this wavelength range [18,25]. The cutback loss curve is in good agreement with the simulated fiber loss [dashed blue line in Fig. 1(b)], which was modeled with Comsol Multiphysics using the finite element method without consideration of the gas absorption inside the fiber. Using the supercontinuum laser and a series of optical filters, the output beam profiles from the output of the 10-m HCF were recorded by a thermal image sensor (Lepton, FLIR) at wavelengths of 3, 3.5, and 4.6 μm. The Gaussian-like beam profiles indicate the delivery of a single-mode beam over the HCF transmission window.

The macrobend loss of the HCF was also investigated, as shown in Fig. 1(c). The transmission spectrum of a 10-m-long fiber at a bend diameter of > 60 cm was recorded as a baseline and then compared with that at bend diameters of 8, 13, 16, 20, and 24 cm. In the fiber's low-loss window, the macrobend loss starts to increase at the short wavelength edge for bend diameters of less than 20 cm. At bend diameters of 13 cm, <1 dB/m macrobend loss was achieved for wavelengths longer than 3.4 μm. The macrobend properties of this HCF make it highly practical for deployment in real-world applications.

The MIR laser used in our pulse delivery experiments was an in-house-built 120-ps optical parametric oscillator (OPO) providing continuous idler wavelength tuning in the range of 2.6–3.6 μm and a maximum average power of 1 W at a repetition rate of 1 MHz, similar to our previous report [26]. The corresponding maximum peak power and pulse energy were 8.3 kW and 1 μJ, respectively. The MIR laser beam quality was good at low output power (< 0.5W, M^2 ~ 1.2) but degraded slightly at higher power to M^2 ~ 1.5 at the maximum power of 1 W. Figure 2 shows the schematic of our MIR HCF power delivery setup. A dichroic mirror (m1) was used to filter out unwanted near-infrared beams (OPO pump and signal beams). Two anti-reflection-coated calcium-fluoride plano–convex lenses (f1, f2; Fig. 2) were used for collimation (f1, f = 250 mm) and then focusing (f2, f = 100 mm) of the MIR beam to ~70 μm diameter in order to match the theoretical fundamental mode field diameter of 73.5 μm for the HCF and to achieve a high coupling efficiency. The HCF was spooled on a 32-cm-diameter drum apart from the two short-end sections, which were held straight to enable input coupling alignment and output beam analysis.

Figure 3(a) shows the power delivered through 5-m and 108-m lengths of the HCF at a wavelength of 3.3 μm. A maximum coupling efficiency of ~70% was calculated by considering the transmission from the 5-m-long fiber and the corresponding

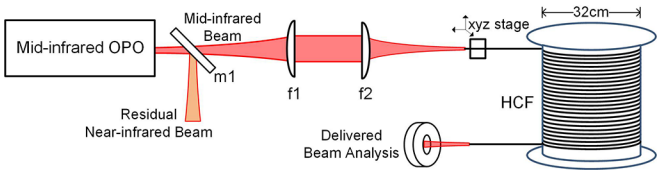

Fig. 2. Schematic of MIR HCF power delivery. Mid-infrared OPO: mid-infrared picosecond optical parametric oscillator; m1: mirror 1; f1: lens 1; f2: lens 2; HCF: hollow-core fiber.

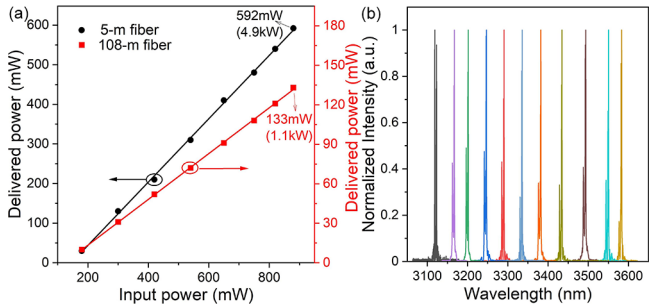

Fig. 3. (a) Delivered versus input average powers through 5-m-long and 108-m-long HCF at a wavelength of 3.3 μm. (b) Tunable delivered MIR laser spectrum through 108-m HCF.

cutback fiber loss. The output power increased linearly with the input power. The coupling did need to be adjusted slightly to optimize the throughput efficiency at higher power levels where the beam quality is lower. For the 5-m and 108-m HCFs, maximum delivered powers (pulse energies) of 592 mW (0.59 μJ) and 133 mW (0.13 μJ) were obtained, respectively, at an input power of 880 mW. The corresponding throughput efficiencies were 67% (5-m fiber) and 15% (108-m fiber), which we believe could be further enhanced by utilizing more advanced low-loss HC-ARF designs, such as conjoined or nested tubes [29,30]. The temporal profile of the MIR laser pulses generated from the OPO was not measured due to the lack of suitable instruments; however, the pulse duration is expected to be similar to that of the OPO pump pulses, which have a Gaussian-like shape and a 120-ps pulse width [26]. For the HCF delivery system, the pulse duration should be maintained through the fiber due to the low dispersion of the HCF (simulated to be 0.2–0.4 ps/nm/km for wavelengths between 3.2 and 3.6 μm) and the relatively narrow pulse spectral bandwidth. The maximum delivered peak powers were therefore estimated to be 4.9 kW and 1.1 kW for the 5-m and 108-m HCFs, respectively.

Several example laser spectra of the 108-m delivered MIR pulses are plotted in Fig. 3(b), as measured by an optical spectrum analyzer (721 series, Bristol Instruments, 1.3–5 μm, 4-GHz resolution). Continuous wavelength tuning is achieved between 3.12 and 3.58 μm, which is difficult to achieve in a long unpurged HCF due to the aforementioned HCl absorption. Note that the multi-peak features of each spectrum (~4 nm spectral linewidth, FWHM) come from the OPO source itself. The long wavelength tuning limit was due to the OPO tuning bandwidth rather than the fiber transmission window [Fig. 1(b)]. In the short 5-m fiber, purging is not essential because the HCl absorption has a much lower impact on the transmission. No nonlinear effects were observed for either HCF length. No laser-induced fiber damage was observed through all of these experiments, indicating that the delivered power was only limited by the available input power in these experiments.

The delivered MIR beams were near diffraction limited; Fig. 4(a) shows the beam quality measurement from the output end of the 108-m HCF at the maximum transmitted power of 3.3 μm. A beam quality of $M_x^2 = 1.02$ and $M_y^2 = 1.03$ was measured using a pyroelectric scanning profiler (NanoScan, Ophir Photonics), and the inset of Fig. 4(a) shows the corresponding output beam profile. The output beam quality from the 5-m fiber was slightly worse, likely due to a small amount of light being transmitted in a higher-order mode over this length scale, but it was still near diffraction limited, with a beam quality of M^2 ~

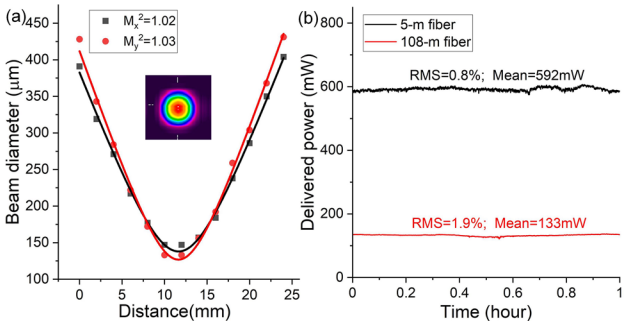

Fig. 4. (a) Beam quality measurements for the 108-m HCF at maximum output power. Inset: the beam profile at the output of the 108-m HCF. (b) Power stability measurements for 5-m and 108-m HCFs over a 1-hour time period at maximum delivered power.

1.1. The delivered laser power stability at the maximum output power for both 5-m and 108-m fibers was recorded for 1 hour, as shown in Fig. 4(b), with corresponding RMS values of 0.8% and 1.9%, respectively. The good power stability is attributed to a number of factors, such as laser power stability, laser pointing stability, and the mechanical stability of the coupling system.

In conclusion, we have demonstrated the first hundred-meter-scale (108-m-long), high-power, near-diffraction-limited MIR pulse delivery system using HC-ARFs. The fiber used has a broad low-loss 2.7–4.7-μm guiding window with minimum fiber loss values of 0.05 and 0.24 dB/m at 3.4–3.6 μm and 4.5–4.6 μm, respectively, with the values at 4.5–4.6 μm representing, to the best of our knowledge, a new record HCF loss at that wavelength. By purging the HCF with argon, parasitic HCl gas absorption was eliminated (at least over a 100-hour observation period). Combining this fiber coiled on a 32-cm-diameter drum with a MIR OPO laser source, tunable MIR laser beams were transmitted at wavelengths from 3.12 to 3.58 μm. Maximum delivered average (peak) powers of 592 mW (4.9 kW) and 133 mW (1.1 kW) were delivered over HCF lengths of 5 m and 108 m, respectively, at a coupling efficiency of ~70%. Such a high-brightness MIR pulse delivery system, offering record delivery distances, could open up new possibilities in terms of MIR devices and approaches, and offers great potential for use in a broad range of industrial, scientific, and medical applications. Further reduction in HCF loss in the mid-IR is to be anticipated in due course with the adoption of more refined fiber designs than used herein.

Funding. Engineering and Physical Sciences Research Council (EP/P027644/1, EP/P030181/1, EP/T020997/1); Royal Society; European Research Council (682724).

Disclosures. The authors declare no conflict of interest.

Data availability. Data underlying the results presented in this paper are available in Ref. [31].

REFERENCES

1. H. C. H. Mulvad, S. Abokhamis Mousavi, V. Zuba, L. Xu, H. Sakr, T. D. Bradley, J. R. Hayes, G. T. Jasion, E. Numkam Fokoua, A. Taranta, S. U. Alam, D. J. Richardson, and F. Poletti, Nat. Photonics **16**, 448 (2022).
2. D. M. Bubb, J. S. Horwitz, R. A. McGill, D. B. Chrisey, M. R. Papantonakis, R. F. H. Jr, and B. Toftmann, Appl. Phys. Lett. **79**, 2847 (2001).
3. V. Z. Kolev, M. W. Duering, B. Luther-Davies, and A. V. Rode, Opt. Express **14**, 12302 (2006).
4. M. Duering, R. Haglund, and B. Luther-Davies, Appl. Phys. A **114**, 151 (2014).
5. K. Johnson, P. Castro-Marin, C. Farrell, I. A. Davidson, Q. Fu, G. T. Jasion, N. V. Wheeler, F. Poletti, D. J. Richardson, and D. T. Reid, Opt. Express **30**, 7044 (2022).
6. K. L. Vodopyanov, *Laser-Based Mid-Infrared Sources and Applications*, (John Wiley & Sons, 2020).
7. J. D. Shephard, A. Urich, R. M. Carter, P. Jaworski, R. R. J. Maier, W. Belardi, F. Yu, W. J. Wadsworth, J. C. Knight, and D. P. Hand, Front. Phys. **3**, 24 (2015).
8. Z. Wang and N. Chocat, Curr. Pharm. Biotechnol. **11**, 384 (2010).
9. G. Tao, H. Ebendorff-Heidepriem, A. M. Stolyarov, S. Danto, J. V. Badding, Y. Fink, J. Ballato, and A. F. Abouraddy, Adv. Opt. Photonics **7**, 379 (2015).
10. S. Qi, Y. Li, Z. Huang, H. Ren, W. Sun, J. Shi, F. Wang, D. Shen, X. Feng, and Z. Yang, Opt. Express **30**, 14629 (2022).
11. S. Sato, K. Igarashi, M. Taniwaki, K. Tanimoto, and Y. Kikuchi, Appl. Phys. Lett. **62**, 669 (1993).
12. D. G. Kotsifaki and A. A. Serafetinides, Opt. Laser Technol. **43**, 1448 (2011).
13. X. Liang, M. Zhong, T. Xu, J. Xiao, K. Jiao, X. Wang, Y. Bin, J. Liu, X. Wang, Z. Zhao, S. Bai, S. Li, D. Du, Y. He, Q. Nie, and R. Wang, J. Lightwave Technol. **40**, 2151 (2022).
14. A. Sincore, J. Cook, F. Tan, A. El Halawany, A. Riggins, S. McDaniel, G. Cook, D. V. Martyshkin, V. V. Fedorov, S. B. Mirov, L. Shah, A. F. Abouraddy, M. C. Richardson, and K. L. Schepler, Opt. Express **26**, 7313 (2018).
15. J. A. Harrington, Fiber Integr. Opt. **19**, 211 (2000).
16. S. G. Johnson, M. Ibanescu, M. Skorobogatiy, O. Weisberg, T. D. Engeness, M. Soljačić, S. A. Jacobs, J. D. Joannopoulos, and Y. Fink, Opt. Express **9**, 748 (2001).
17. N. V. Wheeler, A. M. Heidt, N. K. Baddela, E. N. Fokoua, J. R. Hayes, S. R. Sandoghchi, F. Poletti, M. N. Petrovich, and D. J. Richardson, Opt. Lett. **39**, 295 (2014).
18. F. Yu, P. Song, D. Wu, T. Birks, D. Bird, and J. Knight, APL Photonics **4**, 080803 (2019).
19. R. K. Nubling and J. A. Harrington, Appl. Opt. **35**, 372 (1996).
20. A. Urich, R. R. J. Maier, B. J. Mangan, S. Renshaw, J. C. Knight, D. P. Hand, and J. D. Shephard, Opt. Express **20**, 6677 (2012).
21. A. F. Kosolapov, A. D. Pryamikov, A. S. Biriukov, V. S. Shiryaev, M. S. Astapovich, G. E. Snopatin, V. G. Plotnichenko, M. F. Churbanov, and E. M. Dianov, Opt. Express **19**, 25723 (2011).
22. R. R. Gattass, D. Rhonehouse, D. Gibson, C. C. McClain, R. Thapa, V. Q. Nguyen, S. S. Bayya, R. J. Weiblen, C. R. Menyuk, L. B. Shaw, and J. S. Sanghera, Opt. Express **24**, 25697 (2016).
23. A. N. Kolyadin, A. F. Kosolapov, A. D. Pryamikov, A. S. Biriukov, V. G. Plotnichenko, and E. M. Dianov, Opt. Express **21**, 9514 (2013).
24. A. Urich, R. R. J. Maier, F. Yu, J. C. Knight, D. P. Hand, and J. D. Shephard, Biomed. Opt. Express **4**, 193 (2013).
25. I. A. Davidson, S. Rikimi, H. Sakr, G. T. Jasion, T. D. Bradley, N. V. Wheeler, F. Poletti, and D. J. Richardson, in Specialty Optical Fibers, L. Caspani, A. Tauke-Pedretti, F. Leo, and B. Yang, eds., OSA Technical Digest (Optica Publishing Group, 2020), SoW1H.7.
26. Y. Wu, S. Liang, Q. Fu, T. D. Bradley, F. Poletti, D. J. Richardson, and L. Xu, Opt. Lett. **47**, 3600 (2022).
27. R. Wynne and B. Barabadi, Appl. Opt. **54**, 1751 (2015).
28. T. W. Kelly, P. Horak, I. A. Davidson, M. Partridge, G. T. Jasion, S. Rikimi, A. Taranta, D. J. Richardson, F. Poletti, and N. V. Wheeler, Optica **8**, 916 (2021).
29. F. Poletti, Opt. Express **22**, 23807 (2014).
30. S.-f. Gao, Y.-y. Wang, W. Ding, D.-l. Jiang, S. Gu, X. Zhang, and P. Wang, Nat. Commun. **9**, 2828 (2018).
31. Q. Fu, Y. Wu, I. A. Davidson, L. Xu, G. T. Jasion, S. Liang, S. Rikimi, F. Poletti, N. V. Wheeler, and D. J. Richardson, "Dataset for hundred-meter-scale, kilowatt peak-power, near-diffraction-limited, mid-infrared pulse delivery via low-loss hollow-core fiber," University of Southampton (2022), http://doi.org/10.5258/SOTON/D2361.